Translational Oncology 53 (2025) 102310

Contents lists available at ScienceDirect

Translational Oncology

journal homepage: www.elsevier.com/locate/tranon

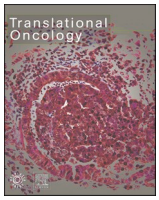

Original Research

CSF3 promotes colorectal cancer progression by activating p65/NF-κB signaling pathway and inducing an immunosuppressive microenvironment

Junfeng Xu [a,1], Na Li [a,b,1], Hui Xie [b,1], Changwei Duan [c], Xingchen Liao [c], Ruoran Li [c], Heng Zhang [c], Yuanming Pan [d], Xianzong Ma [a,b], Shuwen Du [b], Jianqiu Sheng [b], Xin Wang [b,*], Lang Yang [a,b,*], Peng Jin [a,b,*]

[a] Senior Department of Gastroenterology, The First Medical Center of Chinese PLA General Hospital, Beijing 100853, PR China
[b] Department of Gastroenterology, The Seventh Medical Center of Chinese PLA General Hospital, Beijing, 100700, PR China
[c] Medical School of Chinese PLA, Beijing 100853, PR China
[d] Cancer Research Center, Beijing Chest Hospital, Capital Medical University, Beijing 101149, PR China

ARTICLE INFO

Keywords:
CSF3
Colorectal cancer
Ubiquitination
p65/NF-κB signaling
Tumor microenvironment

ABSTRACT

Background: Colony-stimulating factor 3 (CSF3) is a cytokine that promotes inflammation by stimulating the maturation, proliferation, and trafficking of myeloid progenitor cells. However, the functional importance of CSF3 in colorectal cancer (CRC) remains unclear.

Methods: CSF3 expression levels in CRC cells and tissues were detected by quantitative real-time PCR (qRT-PCR), western blot and immunohistochemistry (IHC). *In vitro* and *in vivo* assays were performed to investigate the oncogenic function of CSF3 in the tumor associated malignant phenotypes and the tumorigenic capability of CRC cells. Immunocoprecipitation was performed to verify the regulatory effects of CSF3 on IκBα ubiquitination.

Results: We found that CSF3 was overexpressed in CRC tissues compared to adjacent normal tissues, which correlated with poor patient survival. *In vitro*, silencing CSF3 significantly impaired cell proliferation, colony formation, and migration, while enhancing apoptosis. *In vivo*, silencing CSF3 resulted in reduced tumor growth, weight, and volume, indicating its potential as a therapeutic target. Mechanistically, CSF3 was found to mediate CRC development by activating the NF-κB signaling pathway, as evidenced by the decreased phosphorylation of p65 and reduced IκBα ubiquitination in CSF3-silenced cells. Furthermore, CSF3 silencing modulated immune infiltration in CRC, promoting an anti-tumor immune response and altering the tumor microenvironment.

Conclusion: CSF3 modulated the NF-κB signaling pathway through a distinct mechanism involving p65 phosphorylation and the activation of NF-κB by enhancing IκBα ubiquitination, thereby effectively promoting CRC development, and CSF3 may serve as a potential therapeutic target for repressing CRC advance and metastasis.

Introduction

Colorectal cancer (CRC) is the third most frequently diagnosed and third deadliest cancer type as of 2022 [1]. CRC mortality rates have decreased by approximately 2 % annually over the most recent decade (2010–2019) [1,2]. In addition to population aging and dietary habits, adverse risk factors such as obesity, physical inactivity, and smoking all contribute to an increase in the risk of CRC [3]. Chronic inflammation is also a major risk factor linked to the development of CRC [4]. Current treatments for affected patients include endoscopic and surgical local excision, downstaging preoperative radiotherapy and systemic therapy, extensive surgery for locoregional and metastatic disease, local ablative therapies for metastases, and palliative chemotherapy, targeted therapy and immunotherapy [3]. Although these treatment options have prolonged the overall survival of patients to some extent, the outcomes tend to be less than satisfactory for those with more advanced diseases. A more profound understanding of CRC pathogenesis is likely to result in the development of improved therapeutic strategies.

Granulocyte colony-stimulating factor (G-CSF), now referred to as colony-stimulating factor 3 (CSF3), is an 18–70 kDa glycoprotein, which was first discovered by Metcalf et al. in 1966 [5]. CSF3 is a proinflammatory cytokine with the well-studied function of inducing

* Corresponding authors.
E-mail addresses: wangxin1@301hospital.com.cn (X. Wang), yanglang@301hospital.com.cn (L. Yang), jinpeng@301hospital.com.cn (P. Jin).
[1] These authors have contributed equally to this work.

https://doi.org/10.1016/j.tranon.2025.102310
Received 7 March 2024; Received in revised form 26 December 2024; Accepted 30 January 2025

neutrophil differentiation and mobilization. CSF3 is a growth factor that binds to the CSF3 receptor (CSF3R), thereby activating a complex signal transduction cascade and orchestrating a variety of biological functions, regulating the proliferation, survival, and differentiation of neutrophilic progenitor cells, stimulating the secretion of pro-angiogenic vascular endothelial growth factor, and inducing T cell immune tolerance in stem cell grafts [6]. However, some tumors also express CSF3 and CSF3R, but the significance of CSF3 in CRC remains unclear [7–9].

Here, we found that CSF3 was highly expressed in colorectal tumors. The downregulation of CSF3 suppressed CRC cell phenotypes *in vitro* and *in vivo*. Mechanistically, CSF3 was further determined to regulate the NF-κB signaling pathway by promoting p65 phosphorylation and enhancing IκBα ubiquitination, thereby effectively enhancing CRC tumor growth. Additionally, silencing of CSF3 altered immune cell infiltration in CRC, promoting an anti-tumor immune response and modifying the tumor microenvironment. Our findings suggested that CSF3 exhibited a pro-tumorigenic function in CRC such that further consideration of its potential as a therapeutic target was warranted.

Materials and methods

Cell lines and animals

We purchased human normal colorectal mucosal cell line FHC, CRC cell lines SW480, SW620, RKO, HCT 116 and DLD-1, as well as mouse-derived CRC cells MCA38 from the American Type Culture Collection (ATCC) (https://www.atcc.org/). MCA38, FHC, RKO, HCT 116, and DLD-1 cells were cultured in RPMI-1640 containing 10 % fetal bovine serum (FBS), while SW480 and SW620 cells were cultured in l-15 media containing 10 % FBS. All cells were cultured in a 37 °C incubator with 5 % CO_2.

Four-week-old female BALB/c nude mice and C57BL/6 mice were provided by Cavens Biogle Model Animal Research Co., Ltd. (www.cavens-biogle.cn) and were housed in cages (n = 5/cage) under controlled conditions (22–25 °C; humidity: 50–60 %; and 12 h light/dark cycle) with access to food and water.

Our laboratory animal facility has been accredited by the Association for Assessment and Accreditation of Laboratory Animal Care International, and the Institutional Animal Care and Use Committee of the Seventh Medical Center of Chinese PLA General Hospital approved all animal protocols used in this study. This study was approved by the Ethics Committee of the Seventh Medical Center of Chinese PLA General Hospital.

Tissue sample collection

A CRC tissue microarray (TMA) including 91 CRC samples and 104 para-carcinoma tissues was obtained from the Seventh Medical Center of Chinese PLA General Hospital, Beijing, China. All the patients who provided tissue samples for this TMA signed written informed consent, and none had undergone preoperative interventional therapy or chemotherapy. Detailed clinical data, including age, gender, tumor size, clinical grade, histological type, differentiation degree, and lymph node metastasis, were collected and analyzed for all patients. Invasive adenocarcinoma staging was determined based on analyses of surgically resected specimens using the American Joint Committee on Cancer (AJCC) staging system.

Bioinformatics analyses

CSF3 mRNA levels in CRC and normal tissues were investigated using data from The Cancer Genome Atlas (TCGA) with the GEPIA2 tool (http://gepia2.cancer-pku.cn/#analysis). The co-expressed genes of CSF3 were investigated with the Coexpedia website (https://www.coexpedia.org/search.php). Expression patterns for these co-expressed genes were evaluated in CRC and normal samples from the TCGA database. All obtained differentially expressed genes (DEGs) were subjected to Kyoto Encyclopedia of Genes and Genomes (KEGG) enrichment analyses using the R cluster Profiler package (v 3.16.0).

Immunohistochemical (IHC) staining

Slides were deparaffinized with xylene three times, after which they were subjected to antigen repair using an Ethylene Diamine Tetraacetic Acid (EDTA) solution and blocked using 3 % H_2O_2. Then, primary and secondary antibodies were added, after which DAB and hematoxylin were applied to visualize the expression of antibodies in the healthy and lesion tissue sites. IHC staining was evaluated independently by two pathologists blinded to clinical outcomes. The staining percentage was scored on a scale of 1 to 4, corresponding to increasing staining levels from 1 % to 100 %. Staining intensity was rated from 0 to 3, with 0 indicating no signal and 3 indicating dark brown coloration. IHC scoring included four categories: negative (0), positive (1–4), ++ positive (5–8), or +++ positive (9–12). The IHC scores were used to categorize tissues into high and moderate expression groups based on the median score of all tissues analyzed. Antibodies included anti-CSF3 (1:500, Abcam, #ab204989), anti-Ki67 (1:100, Abcam, #ab16667), anti-F4/80 (1:100, Abcam, #ab204467), anti-CD206 (1:100, Abcam, #ab223961), anti-CD4 (1:100, Abcam, #ab59474), anti-CD8 (1:100, Abcam, #ab237709) and Goat Anti-Rabbit IgG H&L (HRP) (1:400, Abcam, #ab97080).

Plasmid construction and lentiviral transfection

RNA interference was herein used to knock down CSF3. The RNA interference target sequence of CSF3 (shCSF3–1: GTGCTTAGAGCAAGTGAGGAA, shCSF3–2: GCAGATGGAAGAACTGGGAAT, and shCSF3–3: TGCCTCCCATCTGCAGAGC TT) was designed and the corresponding shRNA lentiviral vector was constructed. The scramble sequence (TTCTCCGAACGTGTCACGT) served as negative control (shCtrl). Then, 1.5×10^5 HCT 116 or RKO cells in the logarithmic growth phase were transfected at a lentiviral titer of 3×10^8 TU/mL in the presence of ENI.S + Polybrene, after which they were maintained in RPMI-1640 + 10 % FBS. Transfection efficiency was evaluated using fluorescence microscopy.

RNA extraction and real-time quantitative PCR (qRT-PCR)

Total cell RNA was extracted according to instructions provided with the TRIzol reagent (Sigma, St. Louis, MO, USA), after which it was reverse-transcribed to synthesize cDNA. Then, 10 μL qRT-PCR reactions were prepared with the SYBR Green Mastermixs Kit (Vazyme, Nanjing, Jiangsu, China). Relative gene expression was calculated with the $2^{-\triangle\triangle Ct}$ method. Primer sequences (5′−3′) used for this study included CSF3-forward: CAGAGCCCCATGAAGCTGAT; CSF3-reverse: GCCCTGGATCTTCCTCACTTG; GAPDH-forward: TGACTTCAACAGCGACACCCA; and GAPDH-reverse: CACCCTGTTGCTGTAGCCAAA.

Western blot

The cells were lysed in 1 × Lysis Buffer lysis (Cell Signal Technology, Danvers, MA, USA), the total proteins were separated by 10 % SDS-PAGE prior to transfer onto PVDF membranes, and the membranes were then blocked with TBST solution containing 5 % skim milk at room temperature for 1 h and incubated with primary and secondary antibodies. After that, the membranes were washed with TBST three times (10 min/time), and the ECL+plusTM Western blot system kit was then used for protein band development, followed by the capture of images with X-ray film. Regarding nuclear-cytoplasmic fractionation, cells were harvested and washed with cold phosphate-buffered saline (PBS). The cell pellet was then resuspended in hypotonic buffer containing Tris–HCl (pH 7.4), Nonidet P-40 (NP-40), 10 mM KCl, and protease inhibitors,

followed by gentle rocking on ice for 15 min to allow cell swelling. After centrifugation at 1000 × *g* for 5 min at 4 °C, the supernatant (cytoplasmic fraction) was collected carefully and transferred to a new tube. The remaining nuclear pellet was washed once with hypotonic buffer to remove cytoplasmic contamination. The nuclear pellet was then resuspended in a hypertonic buffer containing Tris–HCl (pH 7.4), NP-40, 0.42 M KCl and protease inhibitors, followed by vortexing to disrupt the nuclear membrane. The suspension was centrifuged at 10,000 × *g* for 10 min at 4 °C to separate the nuclear proteins (in the supernatant) from insoluble debris (pellet). The resulting supernatant containing the nuclear proteins was carefully transferred to a new tube. Both cytoplasmic and nuclear fractions were subjected to protein quantification and subsequent western blot analysis to assess the distribution of specific proteins between the cytoplasm and nucleus. Utilized antibodies included anti-CSF3 (1:500, Abcam, #ab181053), anti-p65 (1:2000, Proteintech, #10,745–1-AP), anti-p-p65 (1:1000, CST, #3033), anti-IκBα (1:1000, CST, #4814S), anti-p-IκBα (1:1000, Abcam, #ab133462), anti-Ubiquitin (1:2000, Santa Cruz, #sc-8017), anti-Histone H3 (1:2000, CST, #4499S), anti-GAPDH (1:30,000, Proteintech, #60,004–1-lg), Goat Anti-Rabbit (1:3000, Beyotime, # A0208), and Goat Anti-Mouse (1:3000, Beyotime, #A0216).

Proliferation assay

After transfection, cells were inoculated in 96-well plates at the density of 2000 cells/well. The CCK-8 assay was used to count the number of cells per well on five continuous days, after which the data were analyzed to plot the cell proliferation curve.

Colony formation assay

After transfection, cells were seeded into a 6-well plate at the density of 5000 cells/well and incubated until colonies containing > 50 cells were visible. Then, the cells were fixed with paraformaldehyde and stained with crystal violet. Colonies were then counted, and their sizes were estimated based on the staining intensity.

Migration assay

Wound healing assays were performed to assess cell migration. After transfection, cells were cultured in 96-well plates (7×10^4 cells/well) and incubated for appropriate periods, after which they were imaged via microscopy. Cell migration rates were calculated based on these images.

Flow cytometry

Lentivirus-transfected cells were cultured in 6-well plates (2 mL/well) for 5 days. Cells were then stained with 5 μL of Annexin V-APC and 5 μL of PI for 10–15 min at room temperature in the dark. Cell apoptosis levels were measured with a FACSCalibur instrument (BD Biosciences, San Jose, CA, USA).

Protein stability assay

For the protein stability assay, cells were treated with cycloheximide (CHX) at a final concentration of 100 μg/mL to inhibit de novo protein synthesis. At various time points (0, 3, 6, and 9 h) post-treatment, cell lysates were prepared and subjected to western blot analysis using antibodies against IκBα and GAPDH. The levels of IκBα were normalized to GAPDH to assess protein degradation over time in HCT 116 and RKO cells transfected with either shCtrl or shCSF3.

Immunoprecipitation for ubiquitination assay

The ubiquitination assay was performed by lysing cells in RIPA buffer containing proteasome inhibitor MG132. Cell lysates were then subjected to immunoprecipitation using an anti-IκBα antibody. The immunoprecipitated protein was resolved by SDS-PAGE and blotted with an anti-ubiquitin antibody to detect ubiquitinated IκBα. The same blots were stripped and reprobed with an anti-CSF3 antibody to confirm the levels of CSF3 in the input lysates. GAPDH was used as a loading control to ensure equal protein loading across samples. This approach allowed us to evaluate the levels of IκBα ubiquitination in HCT 116 and RKO cells under the influence of shCtrl or shCSF3.

Tumor xenograft model establishes

Briefly, 1×10^7 RK0 or MCA38 cells expressing shCtrl or shCSF3 were subcutaneously injected into the axilla of the right forelimb of each mouse ($n = 5$ mice/group). Tumor volume was calculated over time with the formula: volume $= (\pi/6) \times L \times W \times W$, where L and W represented tumor length and width, respectively. After 34 days, the mice were sacrificed, and tumors were removed for weighing and photographing, after which they were frozen in liquid nitrogen and stored at −80 °C. Tumor tissues were collected and analyzed for immune cell infiltration using IHC staining and molecular techniques.

Enzyme-Linked immunosorbent assay (ELISA) for IL-6, TNF-α, IL-10, and TGF-β detection

The levels of IL-6, TNF-α, IL-10, and TGF-β in xenograft tumor tissues were quantitatively measured using respective ELISA kits: the Mouse Interleukin 6 (IL-6) ELISA Kit (Meibiao Biotechnology, #MB-2899A), Mouse Tumor Necrosis Factor α (TNF-α) ELISA Kit (Meibiao Biotechnology, #MB-2868A), Mouse Interleukin 10 (IL-10) ELISA Kit (Meibiao Biotechnology, #MB-2912A) and Mouse Transforming Growth Factor β (TGF-β) ELISA Kit (Meibiao Biotechnology, #MB-6138A) following streamlined protocols. Microplates pre-coated with antibodies for each cytokine were incubated with samples and standards. After the addition of HRP-conjugated detection antibodies and subsequent washing, the colorimetric reaction with TMB substrate was developed and measured at 450 nm. The resulting optical density values were used to determine cytokine concentrations by comparison with a standard curve, providing a concise and reliable assessment of these key inflammatory mediators.

Statistical analysis

All experiments were repeated three times. Data were analyzed using GraphPad Prism 8 (San Diego, CA, USA) and SPSS 19.0 (IBM, SPSS, Chicago, IL, USA). Student's *t*-tests and one-way ANOVAs followed by Tukey's HSD were used to evaluate statistical significance. Data were presented as the mean ± SD. The link between CSF3 levels and clinicopathological characteristics in CRC patients was assessed through Spearman correlation analyses and Mann-Whitney U tests. The survival analysis was determined through Kaplan-Meier survival analyses. A two-tailed $P < 0.05$ was the threshold of significance.

Results

Colorectal cancer patients exhibit significantly increased CSF3 expression

We first characterized CSF3 protein expression levels in CRC through IHC staining of a TMA including 91 tumor tissue samples and 104 normal tissue samples. These analyses revealed that CSF3 expression was significantly enhanced in tumor samples compared with paracancer tissues (Fig. 1A, S1A and Table 1). Furthermore, for the majority of patients included in this CRC TMA, elevated CSF3 levels tended to be associated with poorer patient survival (Fig. 1B). Moreover, we examined the relationship between CSF3 expression and patient clinicopathological parameters. The Mann-Whitney U test indicated that high CSF3 levels tended to be associated with a higher pathological stage, more distant lymphatic metastasis, and more severe lymph node

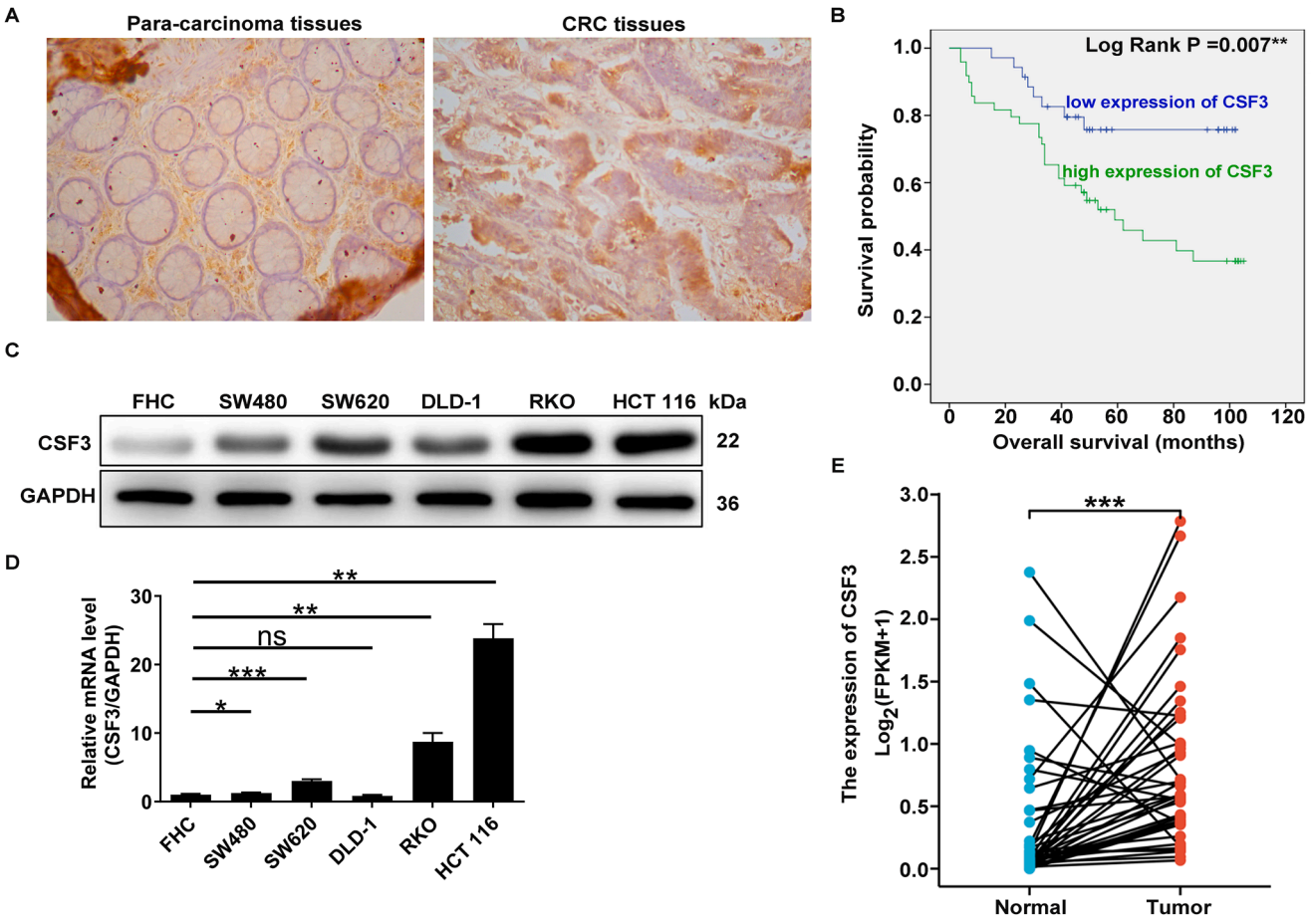

Fig. 1. Colorectal cancer patients show significantly increased CSF3 expression. (A) Representative images of IHC staining showing CSF3 expression between para-carcinoma tissues and CRC tissues. (B) Kaplan-Meier plot illustrating the overall survival probability of CRC patients with low and high expression of CSF3. (C, D) Western blot (C) and qPCR (D) analysis showing the expression levels of CSF3 in normal colorectal mucosal cell line FHC and various colorectal cell lines, including SW480, SW620, DLD-1, RKO, and HCT 116. (E) Scatter plot showing the expression levels of CSF3 in matched CRC and normal samples from TCGA database. * $P < 0.05$, ** $P < 0.01$, *** $P < 0.001$, ns, not significant.

Table 1
Expression patterns of CSF3 in colorectal cancer tissues and para-carcinoma tissues revealed in immunohistochemistry analysis.

CSF3 expression	Tumor tissue		Para-carcinoma tissue		*P* value
	Cases	Percentage	Cases	Percentage	< 0.001
Low	39	42.9 %	93	89.4 %	
High	52	57.1 %	11	10.6 %	

invasion (Table 2), as was also evidenced by Spearman rank correlation analyses (Table 3). Additionally, CSF3 mRNA and protein levels were found to be increased in CRC cells compared to normal FHC cells, with this trend particularly pronounced in HCT 116 and RKO cells (Fig. 1C, D). Subsequent analysis of CSF3 mRNA expression based on RNA sequencing data from The Cancer Genome Atlas (TCGA) dataset confirmed that CSF3 mRNA levels were elevated in CRC patient samples relative to healthy controls (Fig. 1E). These data suggested that elevated CSF3 in CRC was significantly associated with poor overall survival.

Silencing CSF3 affects colorectal cancer cell phenotypes and tumor outgrowth

Next, we aimed to investigate the effects of CSF3 on CRC cell function *in vitro*. Initially, three lentiviruses targeting CSF3 were generated and transfected into HCT 116 cells. The results demonstrated a significant reduction in the relative mRNA level of CSF3 in the shCSF3 groups compared to the shCtrl group, confirming successful knockdown with shCSF3–1, shCSF3–2, and shCSF3–3 (Fig. S1B), with shCSF3–1 and shCSF3–3 being particularly effective. Given the more pronounced effects of shCSF3–1 and shCSF3–3 in silencing CSF3, these were selected for use in the subsequent experiments aimed at excluding off-target effects. Then, shCSF3–1 and shCSF3–3 were transfected into HCT 116 and RKO cells exhibiting high and moderate levels of CSF3 expression. Both qRT-PCR and western blot confirmed a decrease in CSF3 mRNA and protein levels in shCSF3–1 and shCSF3–3 groups (Fig. S1C, D), indicating that CSF3 was effectively silenced by the shCSF3–1 and shCSF3–3 lentiviruses.

Subsequently, CCK-8 assays revealed impaired proliferation of CSF3-depleted HCT 116 and RKO cells (Fig. 2A), further supported by diminished colony formation activity in these CSF3-depleted cells (Fig. 2B). Apoptosis, a critical event in tumorigenesis and progression, was also examined post-CSF3 knockdown using flow cytometry to detect changes in HCT 116 and RKO cell apoptosis. The findings suggested that CSF3 downregulation led to an increase in cell apoptosis (Fig. 2C). In addition to affecting proliferation and apoptosis, we analyzed the abilities of CSF3-depleted HCT 116 and RKO cell migration through wound-healing assay. The results demonstrated that silencing of CSF3 also attenuated the migratory activities of these cells (Fig. 2D). Together, these results indicated that silencing of CSF3 regulated CRC cell phenotypes.

Given the observed effects of CSF3 knockdown *in vitro*, a series of *in vivo* experiments were conducted by establishing a subcutaneous

Table 2
Relationship between CSF3 expression and tumor characteristics in patients with colorectal cancer.

Features	No. of patients	CSF3 expression		*P* value
		low	high	
	91	39	52	
Age (years)				0.014
≤60	47	26	21	
>60	44	13	31	
Gender				0.295
Male	55	26	29	
Female	36	13	23	
Tumor size				0.713
≤4cm	54	24	30	
>4cm	37	15	22	
Differentiation				0.092
low	8	1	7	
medium	81	37	44	
high	2	1	1	
Tumor stage				0.003
I	9	5	4	
II	35	21	14	
III	39	12	27	
IV	8	1	7	
Tumor infiltrate				0.702
T1	1	1	0	
T2	11	5	6	
T3	43	18	25	
T4	36	15	21	
Metastasis				0.071
M0	83	38	45	
M1	8	1	7	
Lymph node invasion				0.014
No	47	26	21	
Yes	44	13	31	
Vascular invasion				0.895
No	86	37	49	
Yes	5	2	3	
Lymphatic metastasis (N)				0.027
0	47	26	21	
1	26	7	19	
2	18	6	12	

Table 3
Relationship between CSF3 expression with patients' age, pathological stage, lymph node invasion and lymphatic metastasis (N).

		CSF3
Age	Spearman correlation	0.260
	Signification (double-tailed)	0.013
	N	91
Stage	Spearman correlation	0.315
	Signification (double-tailed)	0.002
	N	91
Lymph node invasion	Spearman correlation	0.260
	Signification (double-tailed)	0.013
	N	91
Lymphatic metastasis (N)	Spearman correlation	0.233
	Signification (double-tailed)	0.026
	N	91

xenograft model. Briefly, 1×10^7 RKO cells expressing shCSF3 or shCtrl constructs were subcutaneously injected into the axilla of the right forelimb of BALB/c nude mice. We assessed tumor growth indices at the indicated time points and observed a reduction in the volume of tumors in which CSF3 was silenced (Fig. 2E). On day 34 after xenograft tumor inoculation, the mice were sacrificed to harvest tumors. We found that tumor weight and size in shCSF3 group were reduced relative to the shCtrl group (Fig. 2F, G), suggesting that silencing CSF3 could impair CRC tumor outgrowth *in vivo*. To further clarify this possibility, a western blot was performed, and it revealed that CSF3 protein levels were reduced in tumors derived from shCSF3-transfected cells (Fig. 2H). Consistently, IHC staining revealed reduced staining density and intensity for CSF3 and the proliferation marker Ki67 in cell-derived xenograft tumors with shCSF3 (Fig. 2I, J). Taken together, silencing CSF3 could affect CRC cell phenotypes and tumor outgrowth.

CSF3 mediates colorectal cancer development by activating the NF-κB signaling pathway

To elucidate the downstream pathways through which CSF3 mediates CRC development, we utilized the Coexpedia website (https://www.coexpedia.org/search.php) to identify genes co-expressed with CSF3. Genes with a log2 fold change (|log2FC|) greater than log2 and a P-value <3 were identified as differentially expressed genes (DEGs) in CRC and were subjected to Kyoto Encyclopedia of Genes and Gene Set Enrichment analysis (KEGG). The results showed that 12 DEGs were enriched in the NF-κB signaling pathway (Fig. 3A). Importantly, NF-κB signaling pathway has been reported to participate in CRC development [10,11]. P65, a key component of the NF-κB pathway, is known to regulate the activity and transcriptional control of NF-κB [12]. We observed that CSF3 silencing reduced the level of p65 phosphorylation (p-p65) without altering the total p65 protein level (Fig. 3B). To further explore the roles of CSF3 in the regulation of CRC through the NF-κB signaling pathway, we included groups such as shCtrl, shCSF3, shCtrl+PBS, shCSF3+PBS, shCtrl+NF-κB activator (TNF-α), and shCSF3+TNF-α. A series of assays were conducted to assess cell proliferation, colony formation, migration, and apoptosis. The findings indicated that PBS treatment did not significantly affect the outcomes, as anticipated. CSF3 knockdown suppressed cell proliferation, colony formation, and migration while enhancing apoptosis. The addition of TNF-α restored these effects (Fig. 3C-F), highlighting the critical role of the NF-κB pathway in CSF3-mediating CRC development. We also included the following groups: NC, CSF3, NC+PBS, CSF3+PBS, NC+NF-κB inhibitor (Bortezomib), and CSF3+bortezomib (Bortezomib). PBS treatment did not significantly affect the outcomes, as expected. Functional assays showed that CSF3 promoted cell proliferation, colony formation, and migration while inhibiting apoptosis. The addition of the bortezomib (Bortezomib) reversed these effects (Fig. 3G-J), once again demonstrating the critical role of the NF-κB pathway in CSF3-regulating CRC cell events. Western blot analysis was further performed to detect the total and phosphorylated levels of p65. The data revealed that p-p65 was decreased in the shCSF3 group compared to shCtrl group, and increased in the shCtrl+TNF-α and shCSF3+TNF-α groups compared to shCtrl and shCSF3 groups, respectively (Fig. 3K). On the other hand, p-p65 was increased in the CSF3 group compared to NC group and decreased in the NC+bortezomib (Bortezomib) and CSF3+bortezomib (Bortezomib) groups compared to NC and CSF3 groups, respectively (Fig. 3L). Based on these results, we concluded that CSF3 mediated CRC development by activating NF-κB signaling pathway.

CSF3 is involved in the phosphorylation of p65 and the activation of NF-κB by enhancing IκBα ubiquitination

The canonical TLR/NF-κB signaling pathway involves the following process: Activated TLR leads to the recruitment of the IKK complex. The IKK complex consists of IKKγ, IKKα and IKKβ, which then phosphorylate IκBα. Phosphorylation of IκBα leads to its ubiquitination and subsequent degradation by the proteasome. With IκBα degraded, the NF-κB complex is released and can translocate to the nucleus. The NF-κB complex, consisting of P50, p65/c-Rel, binds to the promoter regions of target genes, activating transcription. Our findings revealed that CSF3 knockdown led to a reduction in the phosphorylation levels of p65 (p-p65), without altering the overall p65 protein levels (Fig. 3B). Additionally, we observed an elevation in both p65 and p-p65 within the nucleus upon CSF3 overexpression, as opposed to their cytoplasmic levels (Fig. 4A). This suggested that CSF3 might facilitate the nuclear translocation of

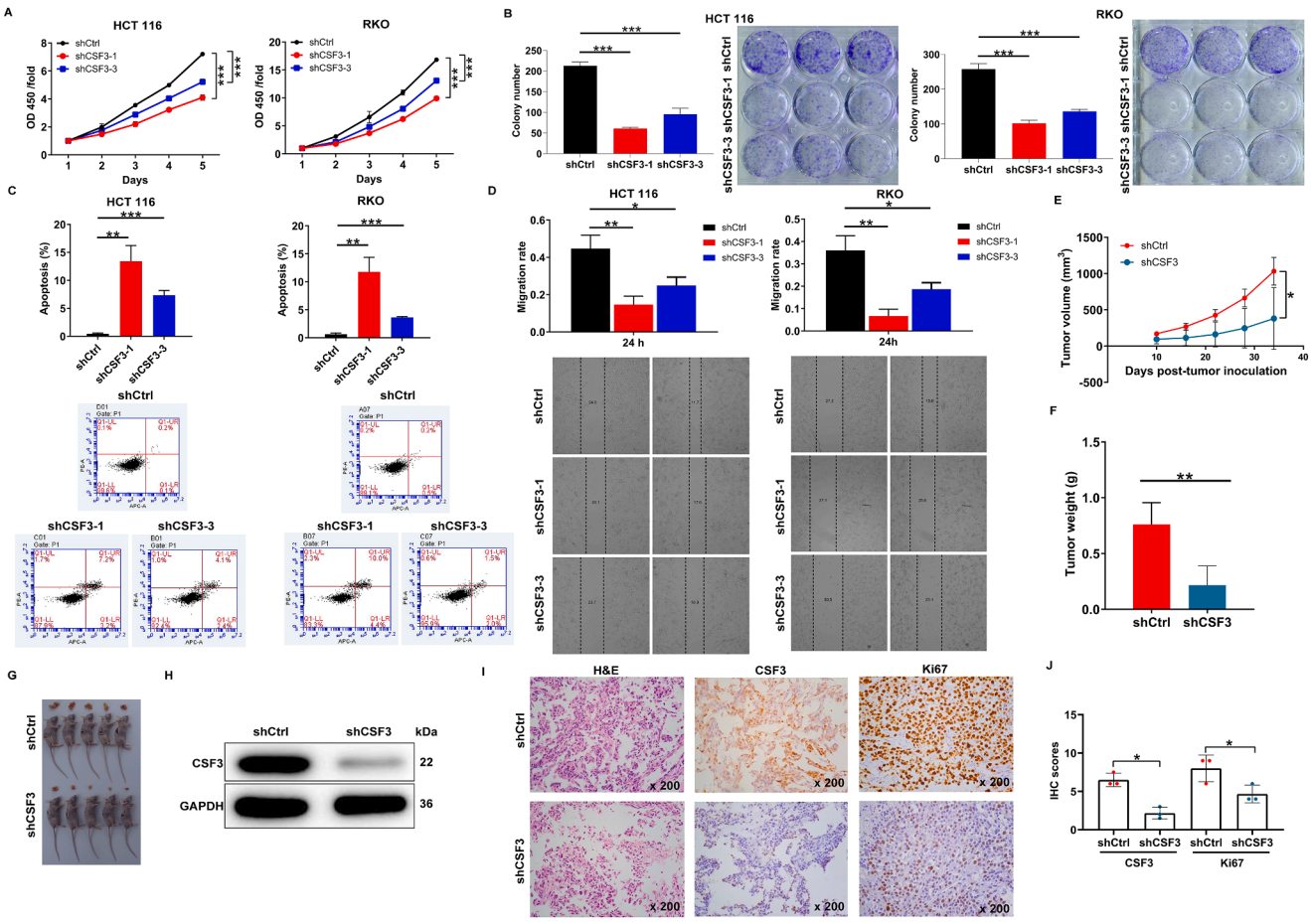

Fig. 2. Silencing CSF3 affects colorectal cancer cell phenotypes and tumor outgrowth. (A) The changes in cell proliferation were assessed via celigo cell counting assay. (B) The abilities to form colony in shCtrl- and shCSF3-transfected HCT 116 and RKO cells were assessed. Individual images were representative of the respective conditions, and each image corresponded to a single well from the same plate. (C) After lentivirus transfection, the abilities of apoptosis were observed via flow cytometry assay. (D) The changes in cell migration were analyzed via wound-healing assays. (E, F) The volume (E) and weight (F) of xenograft tumors derived from RKO cells with shCtrl or shCSF3. (G) The photos of xenograft tumors. (H) CSF3 protein levels were detected in xenograft tumor tissues. (I) H&E staining and IHC analysis of CSF3 and Ki67 antibodies were shown in xenograft tumor tissues. (J) Quantification of IHC staining scores for CSF3 and Ki67. * $P < 0.05$, ** $P < 0.01$. *** $P < 0.001$.

p65. Thus, we hypothesized the involvement of CSF3 in the activation of the NF-κB pathway via IκBα. To address this, we first assessed the levels of total IκBα and phosphorylated IκBα (p-IκBα) in shCtrl and shCSF3-transfected HCT 116 and RKO cells. The results demonstrated that CSF3 knockdown led to a decrease in p-IκBα (Fig. 4B). We then treated cells with cycloheximide (CHX) to block protein synthesis and assessed IκBα degradation in shCtrl and shCSF3 groups. The data showed that the degradation of IκBα was slower in the shCSF3 group (Fig. 4C), suggesting that CSF3 knockdown contributed to the stabilization of IκBα. We further performed immunoprecipitation of IκBα followed by western blot analysis in shCtrl and shCSF3 groups. The findings indicated that the ubiquitination levels of IκBα were reduced in the shCSF3 group (Fig. 4D), further supporting the role of CSF3 in modulating IκBα degradation. These experiments provided evidence that CSF3 was involved in the phosphorylation of p65 and the activation of NF-κB by enhancing IκBα ubiquitination.

CSF3 silencing modulates immune infiltration and tumor microenvironment in colorectal cancer

It is well established that CSF3 can modulate the tumor microenvironment. To assess the impacts of CSF3 silencing on immune infiltration, we established subcutaneous tumor xenograft models using immune-competent C57BL/6 mice. We injected mouse-derived CRC cells MCA38 transfected with shCtrl or shCSF3 and monitored tumor growth. The results showed that CSF3 silencing led to an inhibition in tumor growth, as evidenced by decreased tumor volume and weight (Fig. 5A-C). Moreover, western blot analysis demonstrated downregulation of CSF3 in the shCSF3 group (Fig. 5D). IHC staining further showed decreased CSF3 and Ki67 expression in tumor tissues derived from shCSF3-transfected MCA38 cells (Fig. 5E, F).

Additionally, tumor tissues were collected and analyzed for immune cell infiltration using IHC analysis and molecular techniques. We first quantified the expression levels of M1-type and M2-type macrophage markers in the tumor tissues using ELISA. The results revealed an upregulation of IL-6 and TNF-α in the shCSF3 groups, while the levels of IL-10 and TGF-β were downregulated (Fig. 5G), indicating a shift towards enhanced anti-tumor immune response following CSF3 silencing. Furthermore, IHC analysis revealed that silencing CSF3 led to a decrease in F4/80 and CD206 expression, indicating a reduction in total macrophages and M2-type macrophages, respectively. Conversely, the increase in CD4 and CD8 expression was observed in the shCSF3 group compared to the shCtrl group (Fig. 5H-J), suggesting enhanced infiltration of CD4+ and CD8+ *T* cells into the tumor microenvironment. These findings were consistent with the established role of CSF3 in modulating the immune response in CRC.

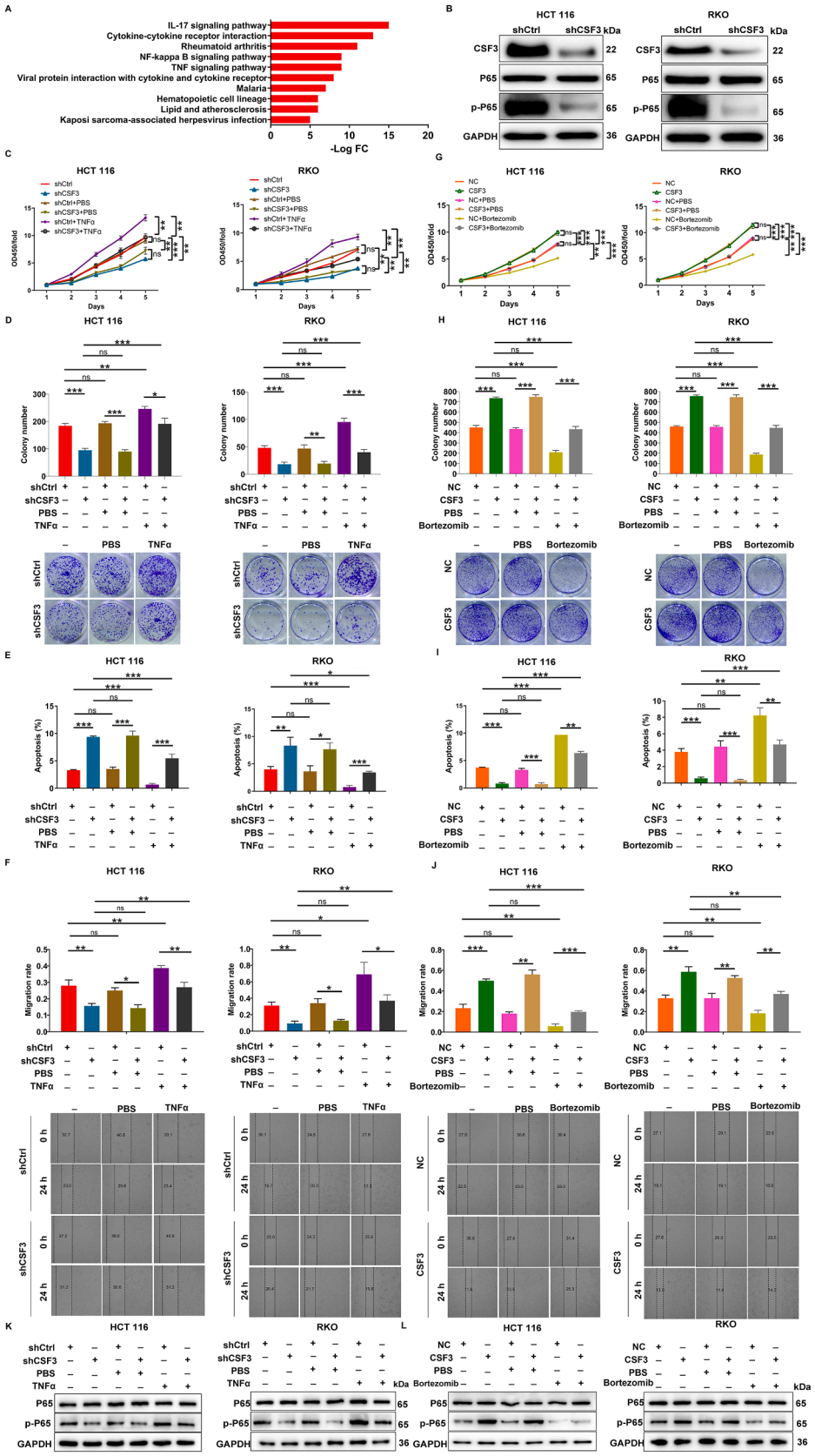

(caption on next page)

Fig. 3. CSF3 mediates colorectal cancer development by activating the NF-κB signaling pathway. (A) KEGG enrichment analysis of CSF3 co-expressed genes. (B) Western blot analysis of CSF3, p65 and p-p65 protein expression in HCT 116 and RKO cells transfected with shCtrl or shCSF3. (C) The results of cell proliferation in HCT 116 and RKO cells transfected with shCtrl or shCSF3, following PBS or TNF-α treatment. (D) The results of colony formation assay in HCT 116 and RKO cells transfected with shCtrl or shCSF3, following PBS or TNF-α treatment. (E, F) Flow cytometry (E) and wound-healing (F) experiments were performed to analyze the changes in cell apoptosis and migration of HCT 116 and RKO cells transfected with shCtrl or shCSF3, following PBS or TNF-α treatment. (G) The results of cell viability in HCT 116 and RKO cells transfected with NC or CSF3, following PBS or bortezomib (Bortezomib) treatment. (H) The results of colony formation assay in HCT 116 and RKO cells transfected with NC or CSF3, following PBS or bortezomib (Bortezomib) treatment. (I, J) Flow cytometry (I) and wound-healing (J) experiments were performed to analyze the changes in cell apoptosis and migration of HCT 116 and RKO cells transfected with NC or CSF3, following PBS or bortezomib (Bortezomib) treatment. (K) Western blot analysis of p65 and p-p65 protein expression in HCT 116 and RKO cells transfected with shCtrl or shCSF3, following PBS or TNF-α treatment. (L) Western blot analysis of p65 and p-p65 protein expression in HCT 116 and RKO cells transfected with NC or CSF3, following PBS or bortezomib (Bortezomib) treatment. "NC" stands for "Negative Control", which refers to the group that was transfected with an empty vector. The "NC" group served as a baseline to compare against the effects of the gene of interest, in this case, CSF3 overexpression.* $P < 0.05$, ** $P < 0.01$, *** $P < 0.001$, ns, not significant.

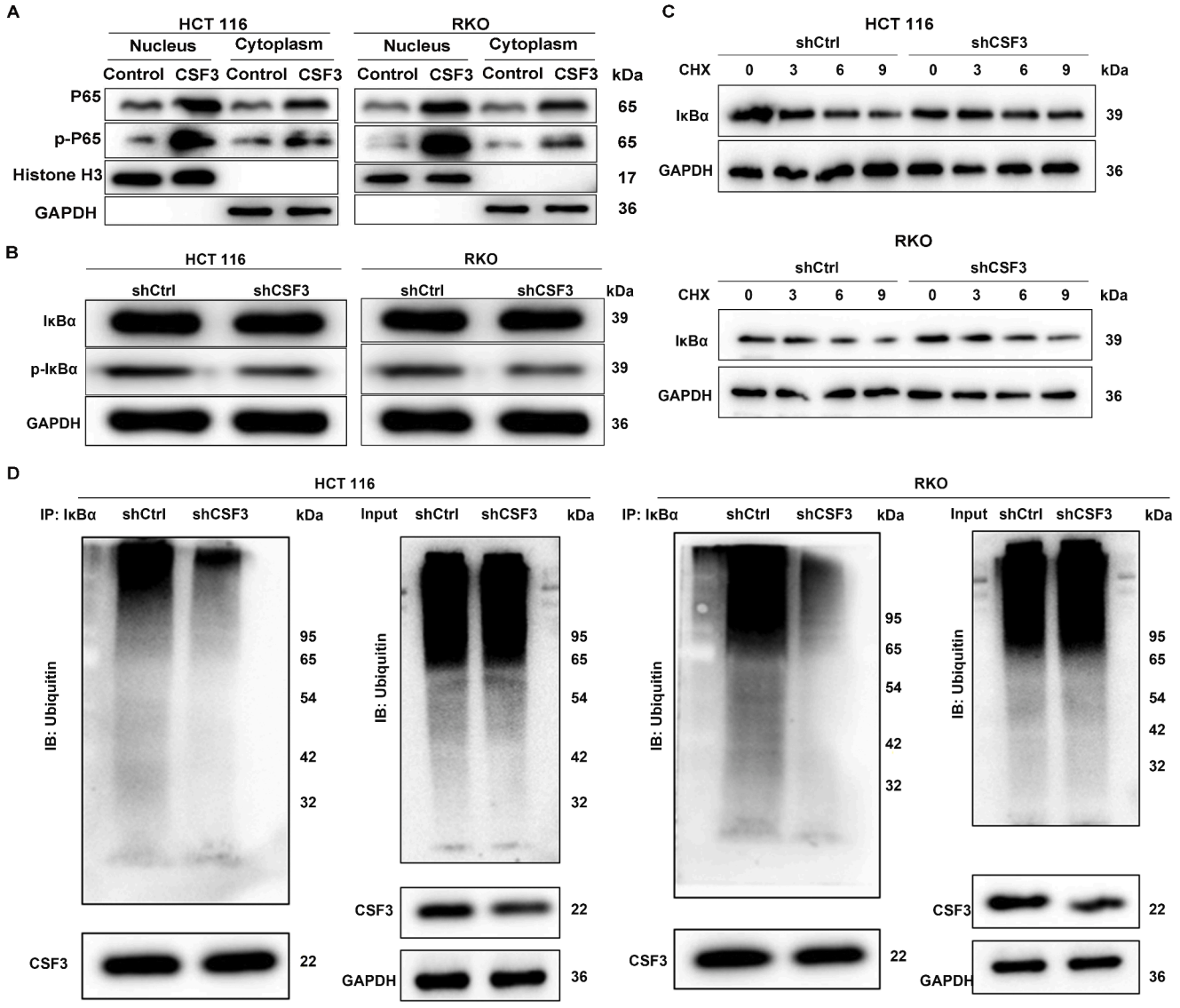

Fig. 4. CSF3 is involved in the phosphorylation of p65 and the activation of NF-κB by enhancing IκBα ubiquitination. (A) Western blot analysis was performed to determine the subcellular distribution of p65, phosphorylated p65 (p-p65), in the nucleus and cytoplasm of HCT 116 and RKO cells with shCtrl and shCSF3. (B) Western blot analysis was used to assess the expression levels of IκBα and phosphorylated IκBα (p-IκBα) in HCT 116 and RKO cells transfected with shCtrl or shCSF3. (C) shCtrl-/shCSF3-transfected HCT 116 and RKO cells were treated with CHX to inhibit protein synthesis, and IκBα protein stability was assessed at 0, 3, 6, and 9 h post-treatment. (D) Cells were lysed, and IκBα was immunoprecipitated using an anti-IκBα antibody. The immunoprecipitated proteins were analyzed by western blot for ubiquitin.

Discussion

In the present study, we identified an important role played by CSF3 in CRC. CRC patients with high levels of CSF3 exhibited decreased overall survival as compared with patients presenting with tumors expressing low CSF3 levels. CSF3 knockdown attenuated CRC cell proliferation and migration while augmenting apoptotic cell death. Our data were consistent with previous reports indicating that CSF3 is

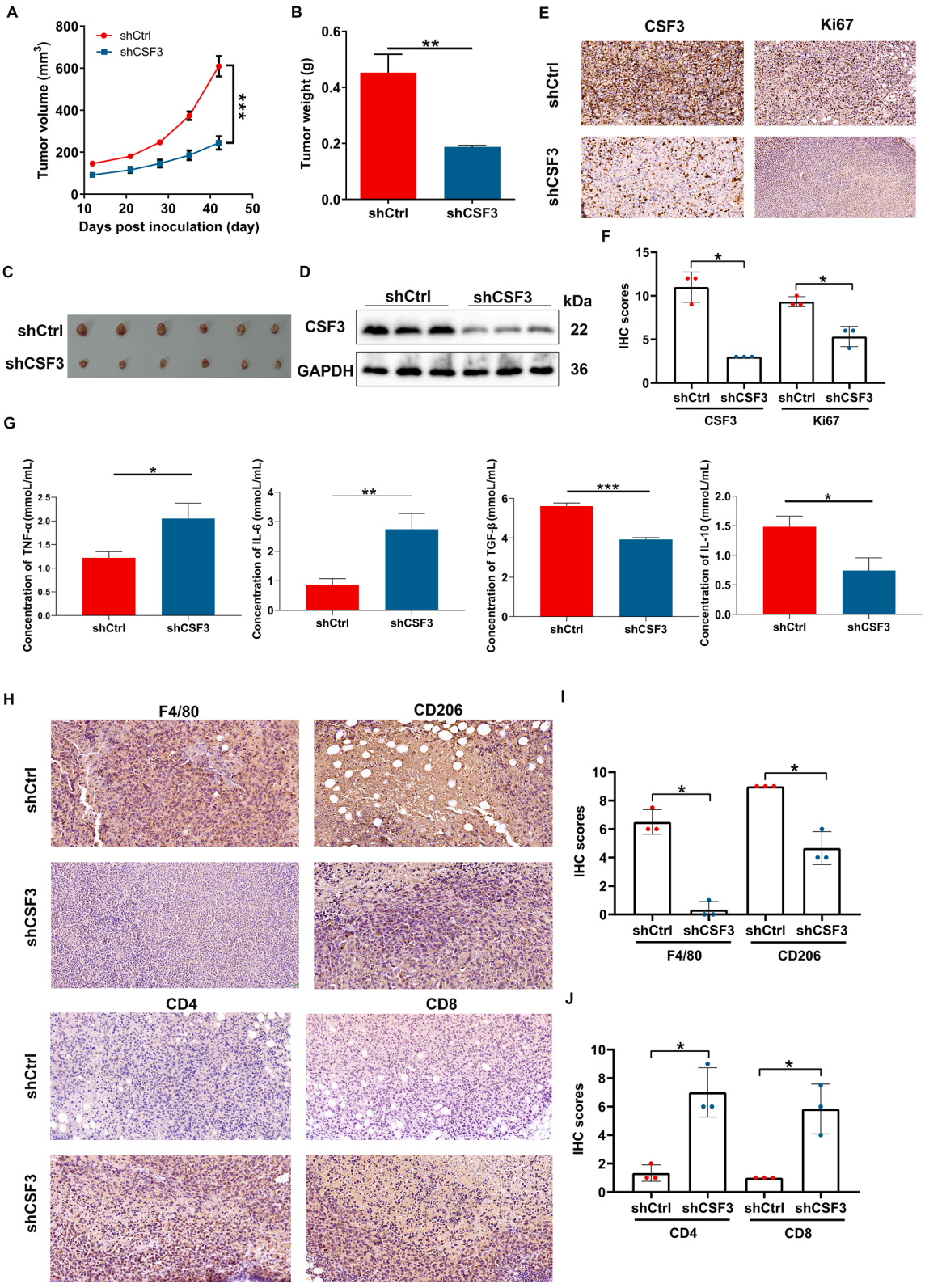

Fig. 5. CSF3 silencing modulates immune Infiltration and tumor microenvironment in colorectal cancer. (A) Graph showing the tumor volume over time in mice inoculated with mouse-derived CRC cells MCA38 transfected with shCtrl or shCSF3. (B) Bar graph representing the average tumor weight in shCtrl and shCSF3 groups. (C) The photos of xenograft tumors. (D) Western blot analysis of CSF3 protein expression in tumor lysates from shCtrl and shCSF3 groups. (E) Representative images of immunohistochemical staining for CSF3 and Ki67 in tumor sections from shCtrl and shCSF3 groups. (F) Quantification of IHC staining scores for CSF3 and Ki67. (G) Bar graphs showing the concentration of M1-type (IL-6 and TNF-α) and M2-type macrophage (IL-10 and TGF-β) markers in tumor tissues as measured by ELISA kit. (H) Representative images of F4/80, CD206, CD4 and CD8 expression in tumor tissues by IHC. (I, J) Quantification of F4/80, CD206, CD4 and CD8 expression in tumor tissues by IHC. * $P < 0.05$, ** $P < 0.01$, *** $P < 0.001$.

responsible for human cancer development [13–15]. CSF3 overexpression has carcinogenic effects in other human cancers. For instance, CSF3 regulates macrophage phenotypes and is associated with poor overall survival in human triple-negative breast cancer [13]. In addition, high levels of tumor-derived G-CSF have been reported in some sporadic cases of aggressive human tumors, and more recent reports have observed high G-CSF and G-CSFR expression in colon and gastric tumors, with CSF3 promoting carcinoma cell proliferation and migration [14,15]. On the other hand, drugs targeting CSF3 have been in clinical use for two decades to stimulate neutrophil and macrophage production and function, particularly in cancer patients. G-CSF, for example, was registered in the USA in 1991 for use in the prophylactic treatment of febrile neutropenia in cancer patients following chemotherapy [16]. Our study revealed that CSF3 expression levels could serve as a novel biomarker for predicting treatment response and prognosis in CRC. The distinct effects of CSF3 on cell growth, colony formation, and apoptosis, as compared to other cancer types, underscore its potential as a specific therapeutic target in CRC.

Unlike previous investigations that primarily focused on the correlation between CSF3 expression and clinical outcomes, our study explored the molecular pathways regulated by CSF3. It was demonstrated that CSF3 signaling is intricately linked to the activation of NF-κB. NF-κB is a ubiquitous transcription factor that mediates a cytoplasmic/nuclear signaling pathway and regulates gene expression of various cytokines, cytokine receptors, and adhesion molecules involved in inflammatory and immune responses [17,18]. Furthermore, there is a correlation between the activation of NF-κB and the control of apoptotic signaling, cell proliferation, differentiation, migration, angiogenesis, and resistance to chemo/radiotherapy in tumor cells [19]. NF-κB is also engaged in tumorigenic processes and cancer survival in a variety of solid tumors including breast cancer, ovarian cancer, prostate cancer, gastric carcinoma, and pancreatic cancer [20–24].

Here, we found that the co-expressed genes of CSF3 were associated with the NF-κB signaling pathway. In addition, CSF3 downregulation resulted in the reduced phosphorylation of the NF-κB subunit. A substantial body of evidence has demonstrated that the NF-κB signaling pathway is involved in CRC development and progression [10,11]. For instance, MyD88 has been shown to function as a potential promotor of CRC through mechanisms mediated by the NF-κB signaling pathway [25]. In addition, B7-H3 overexpression in CRC can promote CRC angiogenesis by activating the NF-κB pathway [9]. SREBP1 can further promote CRC cell invasion and angiogenesis in a manner accompanied by the phosphorylation of NF-κB-p65 [26]. Other studies have demonstrated that DHX9 enhances the phosphorylation of p65 and promotes its nuclear translocation, thereby facilitating NF-κb-mediated transcriptional activity and contributing to malignant CRC phenotypes [27]. This study demonstrated that CSF3 modulated the NF-κB signaling pathway through a distinct mechanism involving p65 phosphorylation and the activation of NF-κB by enhancing IκBα ubiquitination, thereby effectively promoting CRC development.

These findings also indicated that CSF3 not only affected cell proliferation and survival but also modulated the immune cell composition within the tumor microenvironment, which could have significant implications for the development of targeted therapies in CRC. Moreover, the findings suggested that CSF3 could be utilized for patient stratification, allowing for personalized treatment approaches. Patients with high CSF3 expression may benefit from therapies targeting the NF-κB pathway, while those with low expression might require alternative treatment strategies. This stratification has the potential to improve treatment outcomes and reduce unnecessary side effects associated with non-targeted therapies.

Our study complemented the existing body of work by elucidating the precise molecular mechanisms through which CSF3 contributes to CRC progression and by highlighting its potential as a therapeutic target. We believed that these novel findings could advance the field by providing a more nuanced understanding of CSF3's role in CRC.

Conclusion

Our findings demonstrated that CSF3 was upregulated in CRC and promoted CRC cell proliferation and migration through NF-κB pathway, implying that CSF3 might be a potential therapeutic target for CRC.

Data availability

The data generated and analyzed during the present study are available from the corresponding author upon reasonable request.

Ethical statement

All clinical samples were collected with the informed consent of patients. The IACUC (Institutional Animal Care and Use Committee) of the Seventh Medical Center of Chinese PLA General Hospital approved all animal protocols used in this study. This research was approved by the ethics committee of the Seventh Medical Center of Chinese PLA General Hospital (no.2022–89).

Consent for publication

Not applicable.

Funding

This work was supported by National Natural Science Foundation of China (82302914, and 82372939), Beijing Municipal Science and Technology Commission (D171100002617001) and Special Project for Military Medical Innovation (18CXZ027).

Fig. S1 (A) Box plot showing the IHC scores of CSF3 in paracarcinoma and tumor tissues. (B) Bar graphs depicting the relative mRNA levels of CSF3 in HCT 116 and RKO cells transfected with shCtrl or shCSF3 constructs (shCSF3–1, shCSF3–2 and shCSF3–3). (C, D) qPCR and western blot analysis of CSF3 mRNA (C) and protein (D) expression in HCT 116 and RKO cells transfected with control (CON), shCtrl, or different shCSF3 constructs (shCSF3–1, shCSF3–2, shCSF3–3). ** $P < 0.01$, *** $P < 0.001$, ns, not significant.

CRediT authorship contribution statement

Junfeng Xu: Writing – original draft, Visualization, Methodology, Funding acquisition, Formal analysis, Data curation, Conceptualization. **Na Li:** Visualization, Software, Formal analysis, Data curation. **Hui Xie:** Validation, Supervision, Resources, Data curation. **Changwei Duan:** Software, Data curation. **Xingchen Liao:** Validation, Data curation. **Ruoran Li:** Supervision, Resources. **Heng Zhang:** Validation, Formal analysis. **Yuanming Pan:** Supervision, Methodology. **Xianzong Ma:** Investigation. **Shuwen Du:** Software. **Jianqiu Sheng:** Writing – review & editing, Funding acquisition. **Xin Wang:** Validation, Supervision, Methodology, Conceptualization. **Lang Yang:** Writing – review & editing, Visualization, Methodology, Formal analysis, Data curation. **Peng Jin:** Writing – review & editing, Visualization, Resources, Project administration, Methodology, Investigation, Formal analysis, Conceptualization.

Declaration of competing interest

The authors declare that they have no known competing financial interests or personal relationships that could have appeared to influence the work reported in this paper.

Acknowledgements

We thank LetPub (ww w.letpub.com) for its linguistic assistance during the preparation of this manuscript.

Supplementary materials

Supplementary material associated with this article can be found, in the online version, at doi:10.1016/j.tranon.2025.102310.

References

[1] R.L. Siegel, K.D. Miller, H.E. Fuchs, A. Jemal, Cancer statistics, 2022, CA Cancer J. Clin. 72 (1) (2022) 7–33.

[2] F. Baidoun, K. Elshiwy, Y. Elkeraie, Z. Merjaneh, G. Khoudari, M.T. Sarmini, M. Gad, M. Al-Husseini, A. Saad, Colorectal cancer epidemiology: recent trends and impact on outcomes, Curr. Drug Targets 22 (9) (2021) 998–1009.

[3] E. Dekker, P.J. Tanis, J. Vleugels, P.M. Kasi, M.B. Wallace, Colorectal cancer, Lancet 394 (10207) (2019) 1467–1480.

[4] C.D. Gillen, R.S. Walmsley, P. Prior, H.A. Andrews, R.N. Allan, Ulcerative colitis and Crohn's disease: a comparison of the colorectal cancer risk in extensive colitis, Gut 35 (11) (1994) 1590–1592.

[5] D. Metcalf, The colony-stimulating factors and cancer, Nat. Rev. Cancer 10 (6) (2010) 425–434.

[6] L.J. Bendall, K.F. Bradstock, G-CSF: from granulopoietic stimulant to bone marrow stem cell mobilizing agent, Cytok. Growth Factor Rev 25 (4) (2014) 355–367.

[7] E.B. Ninci, T. Brandstetter, I. Meinhold-Heerlein, H. Bettendorf, D. Sellin, T. Bauknecht, G-CSF receptor expression in ovarian cancer, Int. J. Gynecol. Cancer 10 (1) (2000) 19–26.

[8] K. Hirai, M. Kumakiri, S. Fujieda, H. Sunaga, L.M. Lao, Y. Imamura, K. Ueda, M. Fukuda, Expression of granulocyte colony-stimulating factor and its receptor in epithelial skin tumors, J. Dermatol. Sci. 25 (3) (2001) 179–188.

[9] R. Wang, Y. Ma, S. Zhan, G. Zhang, L. Cao, X. Zhang, T. Shi, W. Chen, B7-H3 promotes colorectal cancer angiogenesis through activating the NF-κB pathway to induce VEGFA expression, Cell Death Dis. 11 (1) (2020) 55.

[10] M. Patel, P.G. Horgan, D.C. McMillan, J. Edwards, NF-κB pathways in the development and progression of colorectal cancer, Transl. Res. 197 (2018) 43–56.

[11] A. Soleimani, F. Rahmani, G.A. Ferns, M. Ryzhikov, A. Avan, S.M. Hassanian, Role of the NF-κB signaling pathway in the pathogenesis of colorectal cancer, Gene 726 (2020) 144132.

[12] T. Valovka, M.O. Hottiger, p65 controls NF-κB activity by regulating cellular localization of IκBβ, Biochem. J. 434 (2) (2011) 253–263.

[13] M. Hollmén, S. Karaman, S. Schwager, A. Lisibach, A.J. Christiansen, M. Maksimow, Z. Varga, S. Jalkanen, M. Detmar, G-CSF regulates macrophage phenotype and associates with poor overall survival in human triple-negative breast cancer, Oncoimmunology 5 (3) (2016) e1115177.

[14] M. Toyoda, K. Chikamatsu, K. Sakakura, Y. Fukuda, K. Takahashi, M. Miyashita, K. Shimamura, N. Furuya, A case of squamous cell carcinoma of the head and neck producing granulocyte-colony stimulating factor with marked leukocytosis, Auris Nasus Larynx 34 (2) (2007) 267–271.

[15] K.T. Morris, H. Khan, A. Ahmad, L.L. Weston, R.A. Nofchissey, I.V. Pinchuk, E. J. Beswick, G-CSF and G-CSFR are highly expressed in human gastric and colon cancers and promote carcinoma cell proliferation and migration, Br J. Cancer 110 (5) (2014) 1211–1220.

[16] M. Hansson, T. Söderström, The colony stimulating factors, Med. Oncol. Tumor Pharmacother. 10 (1–2) (1993) 5–12.

[17] P.A. Baeuerle, T. Henkel, Function and activation of NF-kappa B in the immune system, Annu. Rev. Immunol. 12 (1994) 141–179.

[18] Q. Li, I.M. Verma, NF-kappaB regulation in the immune system, Nat. Rev. Immunol. 2 (10) (2002) 725–734.

[19] A.S. Baldwin, Control of oncogenesis and cancer therapy resistance by the transcription factor NF-kappaB, J. Clin. Invest. 107 (3) (2001) 241–246.

[20] Y. Tan, R. Sun, L. Liu, D. Yang, Q. Xiang, L. Li, J. Tang, Z. Qiu, W. Peng, Y. Wang, et al., Tumor suppressor DRD2 facilitates M1 macrophages and restricts NF-κB signaling to trigger pyroptosis in breast cancer, Theranostics 11 (11) (2021) 5214–5231.

[21] W. Yang, L. Liu, C. Li, N. Luo, R. Chen, L. Li, F. Yu, Z. Cheng, TRIM52 plays an oncogenic role in ovarian cancer associated with NF-kB pathway, Cell Death Dis. 9 (9) (2018) 908.

[22] D. Ren, Q. Yang, Y. Dai, W. Guo, H. Du, L. Song, X. Peng, Oncogenic miR-210-3p promotes prostate cancer cell EMT and bone metastasis via NF-κB signaling pathway, Mol. Cancer 16 (1) (2017) 117.

[23] S. Olga, N. Michael, NF-κB signaling in gastric cancer, Toxins (Basel) 9 (4) (2017) 119.

[24] L. Wang, W. Zhou, Y. Zhong, Y. Huo, P. Fan, S. Zhan, J. Xiao, X. Jin, S. Gou, T. Yin, et al., Overexpression of G protein-coupled receptor GPR87 promotes pancreatic cancer aggressiveness and activates NF-κB signaling pathway, Mol. Cancer 16 (1) (2017) 61.

[25] G. Zhu, Z. Cheng, Y. Huang, W. Zheng, S. Yang, C. Lin, J. Ye, MyD88 mediates colorectal cancer cell proliferation, migration and invasion via NF-κB/AP-1 signaling pathway, Int. J. Mol. Med. 45 (1) (2020) 131–140.

[26] Y. Gao, X. Nan, X. Shi, X. Mu, B. Liu, H. Zhu, B. Yao, X. Liu, T. Yang, Y. Hu, et al., SREBP1 promotes the invasion of colorectal cancer accompanied upregulation of MMP7 expression and NF-κB pathway activation, BMC Cancer 19 (1) (2019) 685.

[27] contributes to the malignant phenotypes of colorectal cancer via activating NF-κB signaling pathway, Cell. Mol. Life Sci. 78 (24) (2021) 8261–8281.